

High Power Mid-Infrared Quantum Cascade Lasers Grown on Si

Steven Slivken, Nirajman Shrestha and Manijeh Razeghi *

Center for Quantum Devices, Department of Electrical and Computer Engineering, Northwestern University, Evanston, IL 60208, USA

* Correspondence: razeghi@northwestern.edu

Abstract: This article details the demonstration of a strain-balanced, InP-based mid-infrared quantum cascade laser structure that is grown directly on a Si substrate. This is facilitated by the creation of a metamorphic buffer layer that is used to convert from the lattice constant of Si (0.543 nm) to that of InP (0.587 nm). The laser geometry utilizes two top contacts in order to be compatible with future large-scale integration. Unlike previous reports, this device is capable of room temperature operation with up to 1.6 W of peak power. The emission wavelength at 293 K is 4.82 μm , and the device operates in the fundamental transverse mode.

Keywords: quantum cascade laser; mismatched epitaxy; monolithic integration

1. Introduction

At present, mid-infrared ($3 < \lambda < 5 \mu\text{m}$) semiconductor lasers are primarily sold as individually packaged units. InP-based quantum cascade lasers (QCLs) are a prime example, with access to the entire spectral range and demonstrating records for both output power (200 W) and efficiency (31%) within this band [1,2]. Nevertheless, costs for individual QCLs are still quite high, partly due to the limited number of laser manufacturers and limited number of lasers that can be obtained per wafer. InP substrates typically have a diameter of 100 mm or less, compared to Si, which can reach diameters of 450 mm. State-of-the-art fabrication equipment is also available for larger wafers, which can also improve yield and reduce costs. Therefore, direct production of QCLs on Si has the potential to drastically change the cost per laser and make the technology much more accessible to the general scientific community. The other benefit of this approach is the potential to create custom mi-infrared photonic circuits through massive integration of mid-infrared active optoelectronic components on a low cost photonic platform.

If technically feasible, the most straightforward integration method is the direct epitaxial growth of QCLs on Si wafers. The primary challenge in this case is maintaining the crystalline quality and sharp interfaces of the QCL in the presence of lattice constant and/or thermal expansion mismatch. Si has an 8% lattice constant mismatch and ~50% thermal expansion coefficient mismatch with respect to InP, which is been a significant technical hurdle to overcome. A similar challenge has been tackled in the past for InP-based 1.3–1.55 μm lasers on Si, though, which gives hope that this is possible for QCLs as well [3,4]. In this earlier work, a dislocation density as low as $1.5 \times 10^8 \text{ cm}^{-2}$ was achieved for an InP-on-Si template.

Other groups have attempted this strategy already. Long wavelength ($\lambda > 8 \mu\text{m}$) InAs-based QCLs were demonstrated at room temperature [5]. InP-based QCLs, which would ideally have better performance, have not been as successful, with either only electroluminescence observed [6] or operation up to 170 K at a wavelength of 4.3 μm [7]. Recently, our group made a breakthrough intermediate demonstration of a high power mid-infrared InP-based QCL on GaAs [8], which has approximately half the lattice mismatch (4%) compared to Si. This process continues in this paper, with demonstration of the first strain-balanced, mid-infrared QCL with high power output at room temperature.



Citation: Slivken, S.; Shrestha, N.; Razeghi, M. High Power Mid-Infrared Quantum Cascade Lasers Grown on Si. *Photonics* **2022**, *9*, 626. <https://doi.org/10.3390/photonics9090626>

Received: 8 August 2022

Accepted: 29 August 2022

Published: 1 September 2022

Publisher's Note: MDPI stays neutral with regard to jurisdictional claims in published maps and institutional affiliations.



Copyright: © 2022 by the authors. Licensee MDPI, Basel, Switzerland. This article is an open access article distributed under the terms and conditions of the Creative Commons Attribution (CC BY) license (<https://creativecommons.org/licenses/by/4.0/>).

2. Materials and Methods

In order to grow an InP-based QCL on a Si wafer, a suitable template must be prepared that can transition from the lattice constant of Si to InP and provide a smooth starting surface. For this work, the template was grown entirely by gas-source molecular beam epitaxy (GSMBE).

The starting surface of the template is a (001) 2-inch Si wafer (p-type) that is 4° miscut toward the [110] direction. A 1 µm thick layer of GaAs is deposited at a growth temperature of 600 °C and a growth rate of 0.5 µm/h. Thermal cycle annealing (TCA) is used during this layer to help reduce the dislocation density on the surface [9]. The TCA cycle for this template involves heating to 750 °C during 12 min, annealing for 5 min, and then cooling to 300 °C during 12 min. 6 TCA steps are utilized in total.

Following GaAs growth, a transition is made to InP, with a 100 nm film deposited at 400 °C at a rate of 0.5 µm/h. The wafer temperature is then raised to 570 °C where a 5 nm/ 5 nm Ga_{0.467}In_{0.533}As/ InP superlattice (SL) is used as a dislocation filter [10]. For this template, 5 SL periods are deposited at a time, followed by a 100 nm InP layer. This sequence is repeated 5 times.

Part of the lower contact and waveguide cladding layers are then deposited. This starts with 1 µm of n+ InP ($N_d = 1 \times 10^{18} \text{ cm}^{-3}$) and 50 nm of n+ Ga_{0.467}In_{0.533}As ($N_d = 1 \times 10^{18} \text{ cm}^{-3}$). Next, a 2 µm n- InP layer ($N_d = 2 \times 10^{17} \text{ cm}^{-3}$) and a 1.5 µm n- InP layer ($N_d = 2 \times 10^{16} \text{ cm}^{-3}$) are deposited to finish the template. The template is visually smooth, with a rms roughness of 1.88 nm measured by atomic force microscopy over a 100 µm² area. This is significantly better than the as-grown template demonstrated in Ref. [6] (6.89 nm roughness), but somewhat rougher than the demonstration in Ref. [7] (0.7 nm roughness).

The band structure of the QCL core is based on the shallow-well design in [11], which utilizes a strain-balanced band structure for improved electron confinement. This is also the same core structure used by our group for the demonstration of a high power MWIR QCL on GaAs [8]. Identical layer sequences and environmental conditions are used for growth of a 40-stage, mid-infrared high-efficiency laser core on the InP-coated Si template described above. Growth of the QCL core began with an additional 0.5 µm thick n- InP layer ($N_d = 2 \times 10^{16} \text{ cm}^{-3}$) to complete the lower waveguide cladding. On top of the laser core, a 100 nm thick n-InP layer ($N_d = 2 \times 10^{16} \text{ cm}^{-3}$) is grown, followed by 300 nm thick n-GaInAs ($N_d = 2 \times 10^{16} \text{ cm}^{-3}$) and a 20 nm thick n-InP layer ($N_d = 2 \times 10^{16} \text{ cm}^{-3}$). The wafer is then transferred to a low pressure metalorganic chemical vapor deposition (LP-MOCVD) reactor, where a 3 µm thick n-InP cladding layer (N_d ramped from $2\text{--}20 \times 10^{16} \text{ cm}^{-3}$) and a 1 µm thick n+ InP cap layer ($N_d = 1 \times 10^{19} \text{ cm}^{-3}$) are grown.

The InP-on-Si template has integrated contact layers to facilitate the use of two contacts on the epitaxial (top) side of the wafer. This avoids extra resistance through the heterointerfaces [8] and makes the process inherently compatible with the use of high resistivity Si or silicon-on-insulator (SOI) wafers in the future.

The complete wafer was processed into a buried heterostructure waveguide with a core width of ~17 µm. After chemically etching the waveguide core, semi-insulating Fe-doped InP was regrown around the core using LP-MOCVD. SiO₂ is used as an insulator everywhere except on the very top of the waveguide and in the bottom contact region, which is ~25 µm away from the laser core. Current travels vertically through the laser core from the top contact and laterally from the core to the bottom contact. The Fe-doped InP is used to reduce the lateral waveguide losses due to sidewall scattering at the SiO₂/ Au interface. The contact metal is Ti/Au which is then electroplated with a thick (~2 µm) Au layer. Prior to cleaving the wafer into discrete devices, the Si wafer was thinned to ~65 µm. Oblique and cross-sectional views of a cleaved laser facet, measured by a scanning electron microscope (SEM) are shown in Figure 1. Clear demarcations between the Si substrate, GaAs buffer, and InP-based layers are observed, and the cleaved laser facet is extremely flat near the laser core.

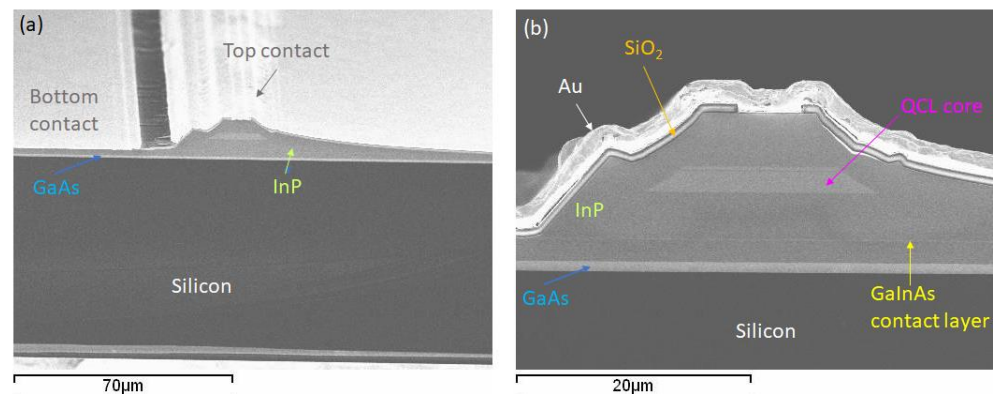


Figure 1. (a) Oblique view of InP-based QCL grown on Si substrate. (b) Closer cross-sectional view of laser cleaved facet.

For testing, an 8 mm long laser bar was cleaved, and some of the lasers had the rear mirror facet high reflection (HR) coated with Y₂O₃/Ti/Au. Laser bars were mounted epilayer-up with indium to copper heat sinks. For cryogenic testing (80–293 K), the laser was placed in a liquid nitrogen cryostat and power was collected through an anti-reflection coated ZnSe window. At temperatures of 293 K and above, the laser heat sink was mounted on a thermoelectric stage, and the temperature was monitored by a thermistor.

Laser testing was done in pulsed mode using 200 ns pulses at a repetition rate of 100 kHz. Average power is measured by a calibrated thermopile detector placed in close proximity to the front laser facet. Peak power is calculated by dividing average power by the pulsed duty cycle (0.02). For uncoated lasers, the total power from both mirror facets is calculated by multiplying the measured power by 2. Spectral measurements are also done in pulsed mode, using a high resolution (0.125 cm⁻¹) Bruker IFS 66v/S FTIR and a deuterated triglycine sulfate (DTGS) detector. For measurements of the laser far field emission, the laser was centered on a rotating stage and measured with a HgCdTe detector with a 1.5 mm aperture at a distance of 30 cm.

3. Results

3.1. Material Characterization of Wafer

Analysis of x-ray diffraction peak full width at half maximum (FWHM) as a function of diffraction angle was used to estimate dislocation density following the method described by Ayers [12]. For the InP/Si template, FWHM data was obtained at multiple diffraction orders for the GaAs and InP peaks. Using the method of the reference, the 1 μm thick GaAs intermediate layer has an estimated dislocation density of $4 \times 10^8 \text{ cm}^{-2}$. The thicker InP layer with the superlattice dislocation filters on top has an estimated dislocation density of $5.3 \times 10^8 \text{ cm}^{-2}$.

After growth of the laser core and upper waveguide cladding, the wafer surface was slightly hazy, with a rms roughness of 9.4 nm over a $100 \mu\text{m}^2$ area. This initial result is still significantly rougher than the value given in Ref. [7] (3.8 nm). Based on cross-sectional SEM measurement, the overall core thickness is ~2% thinner than ideal. The experimental (004) X-ray diffraction spectrum is shown in Figure 2. Distinct peaks are visible in the experimental scan from InP, GaAs, and Si. The QCL core shows a clear superlattice envelope, similar to the simulated spectrum given in the same figure, but the satellite peaks are only weakly observed due to the roughness of the surface and the presence of dislocations. A similar quality X-ray spectrum was observed for a similar structure in Ref. [6].

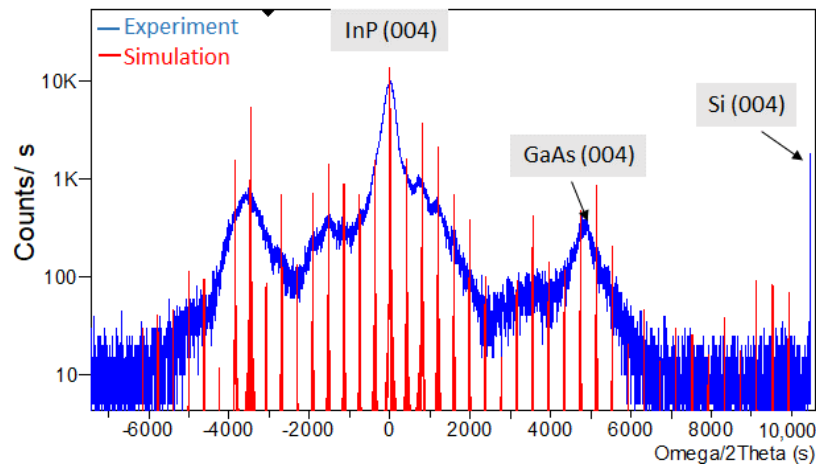


Figure 2. Experimental and simulated (004) diffraction for the strain-balanced QCL grown on Si.

The FWHM of the main InP peak, after growth of upper InP cladding and cap layer by LP-MOCVD was also analyzed by x-ray diffraction at several diffraction orders. While the FWHM (~220 arcsec) was relatively insensitive to diffraction angle, an upper limit for the dislocation density is estimated to be $3 \times 10^8 \text{ cm}^{-2}$.

3.2. Laser Testing Results

Both uncoated and HR-coated lasers show > 1 W peak power output at room temperature, with the HR-coated laser delivering up to 1.6 W, as shown in Figure 3. The threshold current density of the HR-coated and uncoated lasers are 4.2 kA/cm^2 and 4.6 kA/cm^2 , respectively. These values are ~62% greater than the expected values from the laser in Ref. [8]. The variation in threshold current density for the new laser suggests a differential modal gain of ~2 cm/kA, which is also 62% of the value obtained in Ref. [8]. This is extremely promising for an initial result. A more detailed gain/loss analysis was not performed due to the nonlinear nature of the laser power curves above threshold. This is due to the limited operating current range of the lasers tested.

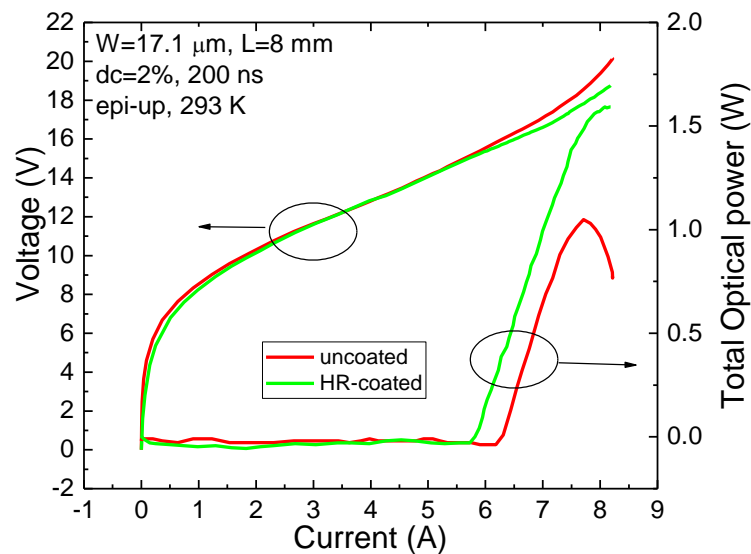


Figure 3. Electrical and output power characteristics for uncoated and HR-coated lasers as a function of current.

The output beam shape in the far field was also measured, as shown in Figure 4. Single lobed emission was demonstrated, which indicates operation in the fundamental transverse

mode. In the direction parallel (perpendicular) to the top wafer surface, the FWHM is 17.4° (49.1°).

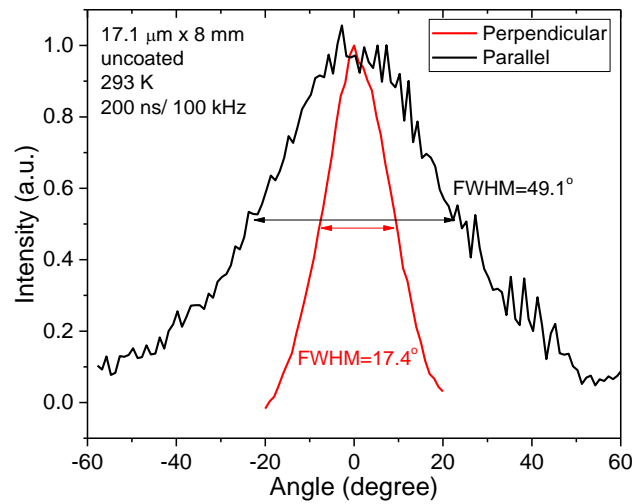


Figure 4. Emission intensity from the laser facet as a function of angle in the far field for directions parallel and perpendicular to the wafer surface.

Laser performance as a function of temperature was also measured, from 80–323 K, as shown in Figure 5. Performance gradually improves as the temperature decreases, with a peak output power up to 4.5 W below 120 K. Threshold current density and slope efficiency are fit exponentially as a function of temperature, as given in Figure 5a. Threshold current density is fit over the whole range, but slope efficiency is only fit from 80–293 K. This was done to avoid a strong deviation near the maximum operating temperature. The main issues observed are a relatively low T_0 and T_1 compared to Ref. [7] (330 K and 709 K, respectively), which indicate a much stronger temperature sensitivity for the laser grown on Si. Nevertheless, room temperature operation is achieved, with projected operation up to ~333 K for the uncoated laser and ~358 K for the HR-coated laser.

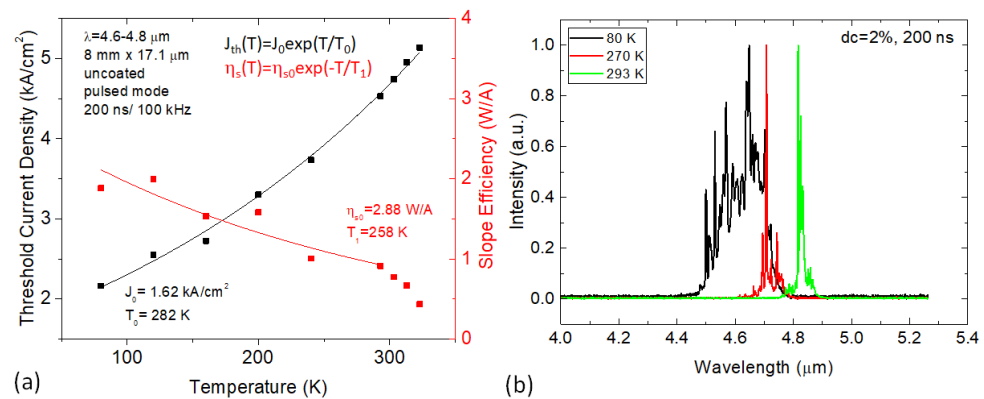


Figure 5. (a) Plot of extracted J_{th} and η_s data as a function of temperature. Solid lines represent exponential fits to the data. (b) Emitting spectra at different operating temperatures.

The emitting spectra for lasers at different operating temperature were also measured. At 80 K, the emission is centered around $\lambda = 4.6 \mu\text{m}$. A red shift is observed at higher temperature, with a room temperature emission wavelength of $4.82 \mu\text{m}$. The emission wavelength matches well to the laser design, and does not show the same shift observed in Ref. [8].

4. Discussion

These results represent a significant improvement over past results [6,7] for mid-infrared QCLs on Si, with about a 180 K increase in operating temperature. However, the current density is generally too high to support continuous wave operation at this time. It is likely that the rougher surface observed on the completed wafer is an indication of a gradual breakdown in the superlattice structure during the laser core growth. This may or may not be influenced by the strain-balanced laser core, in which relaxation may be facilitated by a high dislocation density ($>10^8 \text{ cm}^{-2}$) still present on the wafer surface. The breakdown in the superlattice structure would gradually lead to broadening of the intersubband gain curve and an increase in free carrier absorption within the laser core. In this case, the laser would exhibit a reduced differential gain and increased threshold current density, as seen above. Another consequence of this situation would be a possible decrease in carrier confinement, due a reduced barrier height, which could lead to the lower T_0 and T_1 values observed. Nevertheless, the fact that the laser worked so well in the presence of such a high dislocation density shows some evidence that an intersubband laser may be more tolerant of dislocations than a traditional interband diode laser.

It is clear that some improvement is needed to stabilize the laser core during growth. The first goal is to produce a smoother wafer surface, with fewer dislocations, on which to grow the laser core superlattice. A typical InP-based QCL core has an rms roughness of $<0.2 \text{ nm}$. The QCL on GaAs developed in Ref. [8], which also had very good performance, had an rms roughness of around 2 nm. These are both significantly lower than the 9.4 nm rms roughness exhibited by the current wafer. However, roughness is not the only variable, as the laser from Ref. [7] had roughness of only 3.8 nm but failed to operate above 170 K. This problem needs to be studied further.

Through additional optimization of the InP-on-Si template, laser core growth conditions, and possible modification of the strain level in the laser core, it is expected that the rms roughness of the laser core can be reduced to below 1 nm with a dislocation density in the 10^7 cm^{-2} range. In this case, it is believed that laser performance can be improved significantly.

5. Conclusions

In conclusion, an InP-based, mid-infrared QCL with high peak output power at room temperature has been demonstrated on top of a Si substrate. This was achieved by first developing an InP-on-Si template that can support the two-dimensional growth necessary for intersubband laser operation. Though not yet optimized, further development of the growth technology has a strong potential for higher performance, including continuous wave operation.

Author Contributions: Conceptualization, M.R. and S.S.; investigation, S.S. and N.S.; formal analysis, S.S.; writing—original draft preparation, S.S.; writing—review and editing, N.S. and M.R.; project administration, M.R. All authors have read and agreed to the published version of the manuscript.

Funding: This research received no external funding.

Data Availability Statement: The data presented in this study are available on reasonable request from the corresponding author.

Conflicts of Interest: The authors declare no conflict of interest.

References

1. Heydari, D.; Bai, Y.; Bandyopadhyay, N.; Slivken, S.; Razeghi, M. High brightness angled cavity quantum cascade lasers. *Appl. Phys. Lett.* **2015**, *106*, 091105. [[CrossRef](#)]
2. Wang, F.; Slivken, S.; Wu, D.H.; Razeghi, M. Room temperature quantum cascade laser with 31% wall-plug efficiency. *AIP Adv.* **2020**, *10*, 075012.
3. Razeghi, M.; Defour, M.; Blondeau, R.; Omnes, F.; Maurel, P.; Acher, O.; Brillouet, F.; C-Fan, J.C.; Salerno, J. First cw operation of a $\text{Ga}_{0.25}\text{In}_{0.75}\text{As}_{0.5}\text{P}_{0.5}$ —InP laser on a silicon substrate. *Appl. Phys. Lett.* **1988**, *53*, 2389. [[CrossRef](#)]
4. Shi, B.; Han, Y.; Li, Q.; Lau, K.M. 1.55- μm Lasers Epitaxially Grown on Silicon. *IEEE J. Sel. Top. Q. Electron.* **2019**, *25*, 1900711. [[CrossRef](#)]

5. Loghmari, Z.; Rodriguez, J.-B.; Baranov, A.N.; Rio-Calvo, M.; Cerutti, L.; Meguekam, A.; Bahriz, M.; Teissier, R.; Tournié, E. InAs-based quantum cascade lasers grown on on-axis (001) silicon substrate. *APL Photonics* **2020**, *5*, 041302. [[CrossRef](#)]
6. Rajeev, A.; Shi, B.; Li, Q.; Kirch, J.D.; Cheng, M.; Tan, A.; Kim, H.; Oresick, K.; Sigler, C.; Lau, K.M.; et al. III–V Superlattices on InP/Si Metamorphic Buffer Layers for $\lambda\sim 4.8\ \mu\text{m}$ Quantum Cascade Lasers. *Phys. Status Solidi A* **2019**, *216*, 1800493. [[CrossRef](#)]
7. Go, R.; Krysiak, H.; Fetters, M.; Figueiredo, P.; Suttinger, M.; Fang, X.M.; Eisenbach, A.; Fastenau, J.M.; Lubyshev, D.; Liu, A.W.K.; et al. InP-based quantum cascade lasers monolithically integrated onto silicon. *Opt. Exp.* **2018**, *26*, 22389. [[CrossRef](#)] [[PubMed](#)]
8. Slivken, S.; Razeghi, M. High Power Mid-Infrared Quantum Cascade Lasers Grown on GaAs. *Photonics* **2022**, *9*, 231. [[CrossRef](#)]
9. Yamaguchi, M.; Yamamoto, A.; Tachikawa, M.; Itoh, Y.; Sugo, M. Defect reduction effects in GaAs on Si substrates by thermal annealing. *Appl. Phys. Lett.* **1988**, *53*, 2293. [[CrossRef](#)]
10. Fitzgerald, E.A. Dislocations in strained-layer epitaxy: Theory, experiment, and applications. *Mat. Sci. Rep.* **1991**, *7*, 87. [[CrossRef](#)]
11. Bai, Y.; Bandyopadhyay, N.; Tsao, S.; Slivken, S.; Razeghi, M. Room temperature quantum cascade lasers with 27% wall plug efficiency. *Appl. Phys. Lett.* **2011**, *98*, 181102. [[CrossRef](#)]
12. Ayers, J.E. The measurement of threading dislocation densities in semiconductor crystals by X-ray diffraction. *J. Cryst. Growth* **1994**, *135*, 71. [[CrossRef](#)]